# Optical Bistability by Using a Tunable Fibre Laser with Fibre Fabry–Perot *

LÜ Guo-Hui(吕国辉)[1,2**], YE Hong-An(叶红安)[2], LI Jun-Qing(李俊庆)[1],
SUN Xiu-Dong(孙秀冬)[1], ZHANG Xin-Ming(张昕明)[2]

[1] *Department of Physics, Harbin Institute of Technology, Harbin 150001*
[2] *School of Electronic Engineering, Heilongjiang University, Harbin 150080*

(Received 22 June 2004)

*We observe a novel hybrid optical bistability by using an electro-optically tuned cw fibre laser with a fibre Fabry–Perot filter. The principles of the optical bistable device in two operation manners are analysed. The applications in monitoring the wavelength shift of a tunable fibre laser and fibre sensor of digital type are also discussed.*

*PACS: 42. 65. Pc, 42. 81. −i, 42. 55. Wd*

Because of the compactness and natural compatibility with other fibre components, the fibre devices are widely used in optical communications and fibre sensors. Recently, several studies have focused on the optical bistability (OB) by using the fibre components such as fibre Bragg gratings (FBGs)[2,3] and fibre ring resonator,[4] and applications of the optical bistability in stabilizers of fibre lasers have attracted much attention.[5] As compact devices, fibre Fabry–Perot (FFP) devices provide high-selectivity filters which makes them very attractive for wavelength division multiplexers[6] and tunable fibre lasers because they do not need any additional collimating lenses.

It is well known that a hybrid optical bistable device (OBD) may be constructed by an optical component with nonlinear transmission function and a certain feedback mechanism. To perform the optical bistability, the feedback curve must intersect the nonlinear transmission curve at three places.[1] So far, several OBDs which employ a Fabry–Perot (F-P) interferometer as the modulator have been reported, both intrinsic and hybrid.[7−9] In all these OBDs, the nonlinear transmission curves are obtained by changing the optical path of in the Fabry–Perot device, i.e. adjusting some parameters. Here we propose a novel hybrid OBD in which an FFP is also employed as the modulator, however the nonlinear transmission curve is obtained by changing the wavelength of the incident light using an electro-optically tuned cw fibre laser as the source, rather than by changing the optical path. The device is operated in a spectral domain.

The experimental setup is schematically shown in Fig. 1. In this device, an FBG is employed to construct a resonant cavity of the fibre laser. A weak signal at a certain wavelength controllably selected by the FBG may be amplified in a ring of the erbium-doped fibre (EDF) pumped by a 980-nm laser diode (LD), then may output through two couplers $C_1$ and $C_2$ and with the FFP used as a filter. Two isolators $ISO_1$ and $ISO_2$ are used to confine the light direction. Through an optic-electric conversion circuit, part of the light from $C_2$ is fed back to the PZT attaching an FBG to control the wavelength.

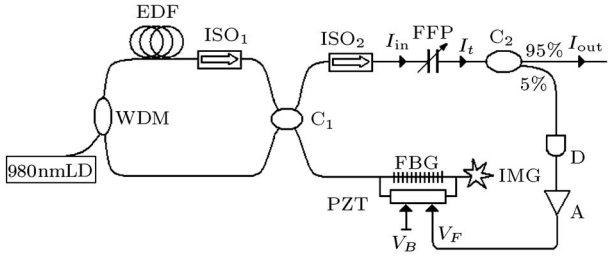


**Fig. 1.** Experimental setup. $C_1$ and $C_2$: couplers, FFP: fibre Fabry–Perot tunable filter, D: photo detector, A: electric amplifier, $ISO_1$ and $ISO_2$: isolators.

The condition of Bragg reflection is $\lambda_B = 2n_{\rm eff}\Lambda$, where $\lambda_B$ is the central wavelength in the FBG reflectance spectrum, $n_{\rm eff}$ is the effective refractive index of the fibre grating, and $\Lambda$ is its period. Any change of $n_{\rm eff}$ or $\Lambda$ will cause a shift of the central wavelength $\lambda_B$. For example, when temperature and strain in the FBG change, $\lambda_B$ will also change, which can be found in the following relation:

$$\frac{\Delta\lambda_B}{\lambda_B} = (1 - p_e)\varepsilon + (\alpha_s + \zeta_s)\Delta T, \qquad (1)$$

where $p_e$, $\alpha_s$, and $\zeta_s$ are the fibre optoelastic coefficient, thermal diffusion coefficient, and the thermo-optical coefficient, respectively. The laser wavelength can be tuned by adjusting the voltage on PZT that causes an axial strain on FBG, and thus induces a shift of the central wavelength of FBG. The transmission curve of the FFP is a function of the wavelength or the voltage on PZT. Here we denote the incident light intensity and the transmissivity light intensity

* Supported by the National Natural Science Foundation of China under Grant No F60077007.
** Email: lvguohui@hlju.edu.cn
©2004 Chinese Physical Society and IOP Publishing Ltd

through FFP as $I_{\rm in}$ and $I_t$, and

$$T = \frac{I_t}{I_{\rm in}} = \frac{(1-R)^2}{(1-R)^2 + 4R\sin(\phi/2)^2}, \qquad (2)$$

$$\phi = 4\pi nL/\lambda, \qquad (3)$$

where $R$ is the reflectivity, $n$ and $L$ is the refractive index and the cavity length of the FFP, $\lambda$ is the wavelength of the incident light in free space. From Eqs. (2) and (3) we can see that instead of changing $n$ and $L$, the nonlinear transmission curve can be obtained by changing $\lambda$, in fact changing the tuning voltage $V$ on PZT in the experiment. The transmission characteristics are studied by measuring the transmissivity $T(V)$ versus the tuning voltage $V$ on PZT, the results are shown in Fig. 2. The transmission curve $T(V)$ of the FFP is a periodic function, but in the context of the problem addressed in this paper only one period of $T(V)$ is concerned. For simplicity of the analysis, we model $T(V)$ as a Gaussian distribution,

$$T(V) = T_0 + \frac{A}{\omega\sqrt{\pi/2}} \exp\Big[-2\frac{(V-V_c)^2}{\omega^2}\Big], \qquad (4)$$

where $\omega = \omega_1/\sqrt{\ln 4}$, $\omega_1$ is the full width at half maximum (FWHM) of the Gaussian distribution; $A$ and $T_0$ are the distribution area and the offset in the Gaussian distribution; $V$ and $V_C$ are the voltage on PZT and the central voltage of the Gaussian distribution. We have $V = V_B + V_F$ with $V_B$ and $V_F$ being the bias voltage and the feedback voltage, respectively. Using Eqs. (4) and choosing $\omega = 11.515$, $A = 7.4113$, $T_0 = 0.019568$, $V_C = 60.273$, we can obtain the fitting curve as shown by the solid line in Fig. 2. It is obvious from Fig. 2 that the Gaussian model works well for the present study, and the curve meets the requirements for exhibiting optical bistability because of possessing extreme and inflexion points.

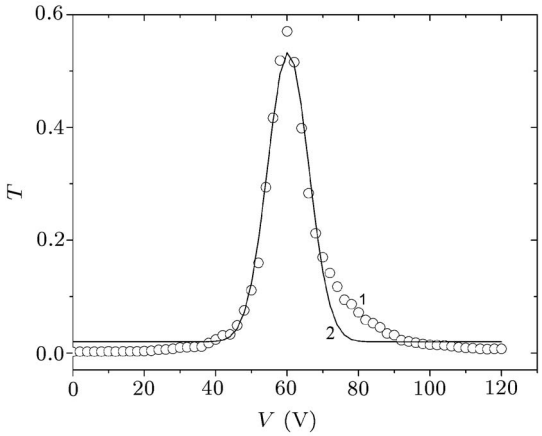


**Fig. 2.** Relationship between transmissivity $T(V)$ and tuning voltage $V$ on PZT. Circles: the experimental results. Solid line: the fitting with Gaussian distribution.

To perform the optical bistability, the initial output wavelength from the laser is adjusted to 1547.8 nm by changing $V_B$, and the peak wavelength of the FFP is shifted to 1548.1 nm with a 7.5 V voltage. The feedback part of the OBD consists of coupler $C_2$, photodetector D and electric amplifier A. The feedback voltage $V_F$ is applied on PZT through a feedback circuit and proportional to coupling ratio of $C_2$ and $I_t$. Therefore the tuning voltage on PZT can be written as

$$V = V_F + V_B = \eta K_2 G I_t + V_B, \qquad (5)$$

where $K_2$, $\eta$, and $G$ are the coupling ratio of $C_2$, conversion efficiency of D and the gain of A, respectively. Really, $K_2 = 5\%$, $\eta = 0.54\,{\rm V/mW}$.

In the $T(V)$–$V$ plane, the feedback can be expressed in the form

$$T(V, I_{\rm in}, V_B) = \frac{I_t}{I_{\rm in}} = \frac{1}{\eta K_2 G I_{\rm in}}(V - V_B) \qquad (6)$$

and

$$I_{\rm out} = (1 - K_2) I_t. \qquad (7)$$

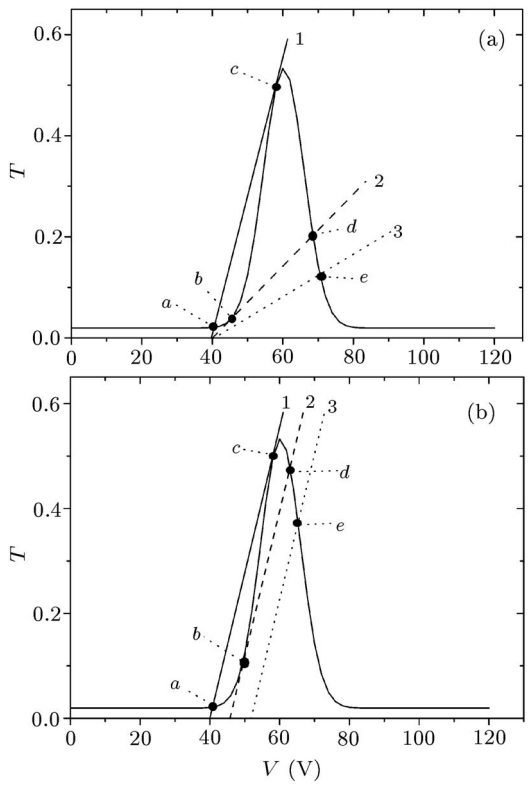


**Fig. 3.** (a) The hysteresis loop formation process by adjusting the input intensity $I_{\rm in}$ (i.e. the slopes of lines 1, 2, 3). Here $V_B$, $G$ and $K_2$ are fixed. When $I_{\rm in}$ increases first and then decreases, correspondingly the feedback curve moves along the direction $1 \to 2 \to 3$ first, and then back to $3 \to 2 \to 1$. In this process, the operating points move along $a \to b \to d \to e$, and then back to the direction of $e \to d \to c \to a$. (b) The hysteresis formation process by changing $V_B$. Here $I_{\rm in}$, $G$ and $K_2$ are kept constant, while $V_B$ increases first and then decreases.

The operating points of the OBD are determined by the solutions of Eqs. (4) and (6), which can also be directly expressed in terms of intersections between the series of feedback lines and transmissivity curve, as shown in Fig. 3. Usually, there are two operation manners to realize bistability: keeping one of $I_{\rm in}$ and $V_B$ fixed and adjusting the other one gradually.

In the first operation manner, as illustrated in Fig. 3(a), $V_B$, $G$ and $K_2$ are fixed. When $I_{\rm in}$ increases first and then decreases, correspondingly the feedback curve moves along the direction $1 \to 2 \to 3$ first, and then back to $3 \to 2 \to 1$. In this process, the operating points move along $a \to b \to d \to e$, and then back to the direction of $e \to d \to c \to a$, forming hysteresis curve as shown in Fig. 4(a). Figure 3(b) shows the second operation manner, where $I_{\rm in}$, $G$ and $K_2$ are kept constant, while $V_B$ increases first and then decreases. The corresponding experimental hysteresis curve is shown in Fig. 4(b). Figure 5 illustrates the calculated results by Eqs. (4), (6) and (7), concentrating on the dependence of the width of the hysteresis loops. In Fig. 5(a), curves 1–4 correspond to $G = 4000$, 5000, 6000 and 7000 respectively, while in Fig. 5(b), curves 1–4 correspond to $G = 1200$, 1400, 1600 and 1800 respectively, and $I_{\rm in} = 1\,{\rm mW}$.

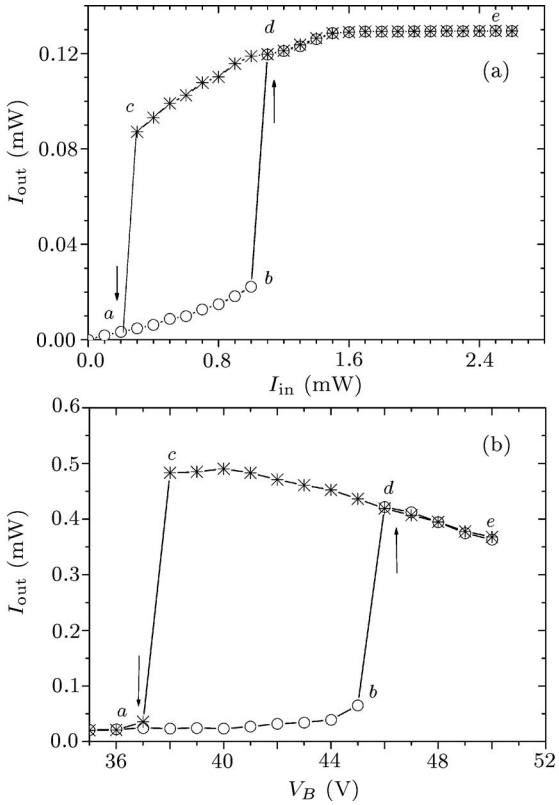


**Fig. 4.** Experimental results, showing hysteresis loops corresponding to Figs. 3(a) and 3(b).

From Fig. 5 we can see that the width of the hysteresis loop become narrower when increasing the gain of the amplifier for the first operating manner. For the second manner, the width of the hysteresis loop becomes narrower when increasing the slope of the feedback line by decreasing $G$.

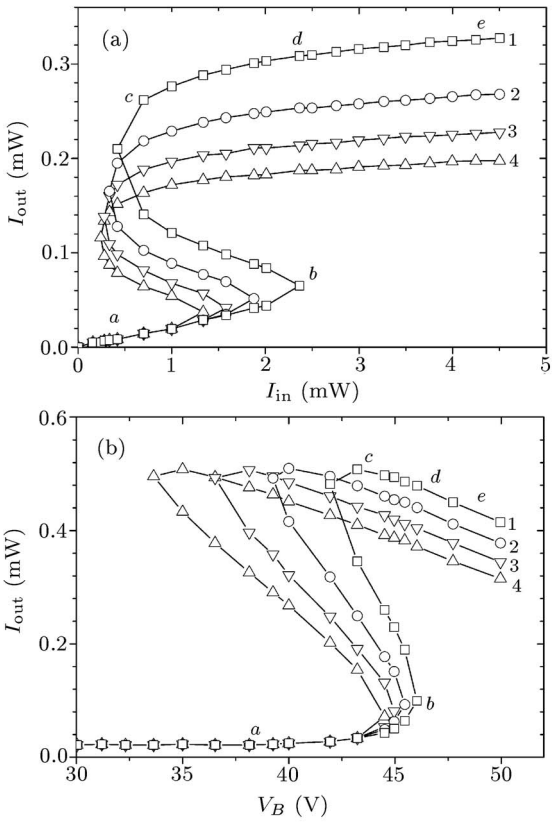


**Fig. 5.** Calculated results by using Eqs. (4), (6) and (7), showing the dependence of the width of the hysteresis loops, corresponding to Figs. 3(a) and 3(b). (a) Curves 1–4 correspond to $G = 4000$, 5000, 6000 and 7000, respectively; (b) curves 1–4 correspond to $G = 1200$, 1400, 1600 and 1800, respectively.

We are interested in the second operation manner because of its potential applications. In this process, the bistable hysteresis loop, as described above, is obtained by adjusting $V_B$, which is in fact due to the shift of the wavelength from the laser. There is existence of a minimum width of the hysteresis loop, which corresponds to the maximum slope of feedback line allowed to have more than two intersections with the transmission curve of the FFP. This minimum hysteresis loop width in wavelength is evaluated as the order of magnitude of 0.0001 nm in our experiment. This means that when the output wavelength of the laser changes about 0.0001 nm, the OBD exhibits a switching process accompanying the producing of an electric pulse, which can be used to monitor the shift in the output wavelength from a laser in a digital way or to trigger the special circuit to compensate for the change in wavelength and hence to lock in the laser wavelength (frequency).

Such an OBD can also be used as an optic-fibre sensor of digital type using this switching phenomenon. When the environment measurand causes a shift of the transmissivity peak wavelength of the FFP of the order of magnitude of 0.0001 nm, which is equivalent to shifting the feedback line by the same amount with changing $V_B$, the OBD will switch ON or OFF as described above. We can not only implement high accuracy measure by counting the number of the pulses but can also distinguish the variation direction of the measurand by judging the sign of the electric pulse. These are the main advantages of this fibre bistable sensor technique.[10]

In conclusion, we have demonstrated the optical bistability in an FFP by using a tunable fibre laser with an FBG. We have also discussed the potential applications of such an OBD.

# References

[1] Gibbs H M 1985 *Optical Bistability: Controlling Light with Light* (New York: Academic)

[2] Li J Q, Chen Q, Li Q H and Li C F 2002 *Chin. Phys. Lett.* **19** 1815

[3] Chao X S 1995 *IEEE J. Quantum Electron.* **31** 2037

[4] Luo L G and Chu P L 1998 *Opt. Commun.* **149** 307

[5] Ye H A, Zhang X M and Zhu Y 2004 *Chin. Phys. Lett.* **21** 860

[6] Beatriz O, Jose C and Jose L C 1999 *J. Lightwave Technol.* **17** 1241

[7] Felber F S and Marburger J H 1976 *Appl. Phys. Lett.* **28** 731

[8] Smith P W, Turner E and Maloney P P 1978 *IEEE J. Quantum Electron.* **14** 207

[9] Li C F and Xu J C 1981 *Acta Opt. Sin.* **1** 167 (in Chinese)

[10] Li C F, Zhou F and Yang K 2002 *J. Nonlin. Opt. Phys. Mater.* **11** 125